Journal of the Korean Physical Society, Vol. 63, No. 6, September 2013, pp. 1189∼1193

Morphology-dependent Optical Properties of One-dimensional Nanostructure-arrayed Silicon

Shao-long Wu, Guo-an Cheng,* Rui-ting Zheng and Xiao-ling Wu
Laboratory of Nanomaterial and Technology, Key Laboratory of Beam Technology and Material Modification of Ministry of Education, College of Nuclear Science and Technology, Beijing Normal University, Beijing 100875, China

(Received 9 April 2013)

The optical properties of one-dimensional nanostructure-arrayed silicon (1DNSASi), which was fabricated by the metal assisted electroless chemical etching method under different conditions, were characterized in the wavelength range of 220 - 1000 nm. Whether the optical absorption of the 1DNSASi was enhanced relative to that of the polished Si was determined from the detailed morphology of the 1D nanostructures. For the yellow 1DNSASi prepared at a high etchant concentration and high temperatures, its optical absorption was relatively nice in the ultraviolet light region, while a gradual attenuation was shown in the visible and the near-infrared regions, and the optical absorption was lower than that of the polished Si at wavelengths above 800 nm. When the effects of zeroth-order reflectance and zero transmission were combined, the optical absorption of the black 1DNSASi prepared at a low etchant concentration and room temperature was very high ($> 99\%$) in the wavelength range of 220 - 1030 nm and displayed a slight decrease at wavelengths above 1030 nm. Our results demonstrate that the optical absorption of the black 1DNSASi could be further improved by increasing the etching depth and exhibited its measurable maximum value when the etching depth was large enough. These results indicate that the 1DNSASi may be a promising candidate for high-efficiency photovoltaic devices, high-sensitivity sensors and detectors.

PACS numbers: 79.60.Bm
Keywords: Morphology dependence, Optical absorption, Reflection suppression, Silicon nanostructure array
DOI: 10.3938/jkps.63.1189

I. INTRODUCTION

Recently, quasi-one-dimensional nanostructures have been being widely researched due to their unique physical, chemical and mechanical properties [1–5]. Because of their high aspect ratio and large surface-to-volume ratio, one-dimensional (1D) nanostructures exhibit promising applications based on individual 1D nanostructure or arrays in photodetectors, photovoltaics, biosensors, chemical sensors and other nanoscale devices [6–10]. Si material is being widely researched and has been applied in theory and practice because of its several beneficial features: 1) Si is plentiful and ubiquitous and is the second most abundant element on earth; 2) Si is usually nontoxic and stable; 3) its band gap is almost ideally-matched to the terrestrial solar spectrum. However, many problems, such as limited photoelectrical conversion efficiency due to the indirect band gap, large device size blocking an improved integration level, too high a cost, high power consumption, and so on, still exist with Si-based optoelectronic devices. Thus preparing Si material with excellent optical absorption properties in a cheap way is very significant. In the past decades, much theoretical [4, 11] and experimental research [1,12] has been carried out to suppress reflections, including coating antireflective films [13], etched textured surfaces [14] and 'moth eye' surfaces [15–17]. Nevertheless, antireflective coatings are usually fabricated by using a vacuum evaporation method and have poor adhesion, fabrication of 'moth eye' surfaces by using conventional methods needs complex and expensive lithography technology, and textured surfaces only have a limited suppression of the optical reflectance in a short spectral range.

Sub-wavelength resonance effects between nanostructures are expected and have been demonstrated to suppress the optical reflectance [18]; therefore, 1D nanostructure-arrayed Si (1DNSASi) has the potential to improve the performances of various Si-based photoelectrical devices [19]. Here, we present the ultralow broadband reflectance of Si covered by 1D Si nanostructure arrays synthesized by metal-assisted chemical etching. Besides, we compare the optical reflection and transmission characteristics of various 1DNSASi with different nanostructure lengths in the spectral range of 220 - 1100 nm. We ascribe the observed behaviors to the

*E-mail: gacheng@bnu.edu.cn; Fax: +86-010-6220-5403

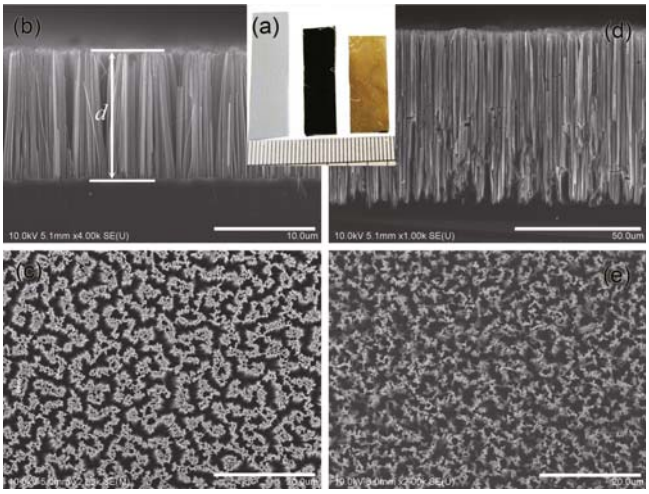

Fig. 1. (Color online) (a) photograph of polished Si (left), black 1DNSASi (middle) and yellow 1DNSASi (right); cross-sectional SEM images of (b) black and (d) yellow 1DNSASi, and top-view SEM images of (c) black and (e) yellow 1DNSASi.

strong trapping of the incident light among the nanostructures, combined with light scattering on the surfaces of the nanostructures.

II. EXPERIMENTS

Vertically-aligned 1D nanostructure-arrayed Si was fabricated directly by etching an n-type Si(100) wafer with a resistivity of 1 - 10 Ωcm. The whole process is relatively simple and low-cost, which is similar to our previously reported technology [20,21]. The detailed process was performed in four steps: 1) Commercial Si wafers were cut to nominal 1 × 2 cm^2, cleaned ultrasonically in de-ionized water, acetone and ethanol for 10 min each, and then immersed in boiling mixed solution of H_2SO_4 (97 wt.%) and H_2O_2 (40 wt.%) in a volume ration of 4:1 for 10 min, this was followed by several washes with de-ionized water and then the samples were stored in de-ionized water for use. 2) As-cleaned Si chips were soaked in a diluted HF (4 wt.%) solution for 2 min to remove the native oxide layer, and then were immersed immediately into a 4 M HF-based aqueous solution containing 0.02 M $AgNO_3$ for 1 min for electroless deposition of Ag nanoparticles (AgNPs). 3) AgNP coated Si chips were soaked in an etching solution composed of a 4 M HF and H_2O_2 for various times at room temperature. The yellow 1DNSASi sample was prepared in 0.4 M H_2O_2 at a 70 °C water bath, and the black ones in 0.2 M H_2O_2 at room temperature (about 15 °C). 4) Finally, the 1DNSASi samples were immersed in boiling 50% HNO_3 for 1 h to remove the residual AgNPs.

The 1DNSASi morphologies were characterized by using a field emission scanning electron microscope (FE-SEM, Hitachi S-4800). Etching depths were determined to digitally analyze the cross-sectional SEM images by using computerized correlations of pixel intensities along lines parallel to the etched surfaces. Reflection and transmission spectra were obtained by using an UV-Vis spectrophotometer equipped with an integrating sphere (SPECORD 200, Analytik Jena AG). Total optical reflectance spectra (R) were measured by illuminating samples at 8° off-normal and integrating the specular and diffuse reflectance. Total transmission spectra (T) were measured by keeping the samples over the opening of the integrating sphere and illuminating them with normal light. The effective absorption (A) was calculated by using A=1 – R – T without correction or other possible losses.

III. RESULTS AND DISCUSSION

Figure 1(a) present photographs of the as-cleaned Si chip and of the two kinds of 1DNSASi prepared in different conditions. The diverse colors indicate their morphologies and optical reflectance properties are discriminating. For the black 1DNSASi, the internal distances between adjacent nanostructures ranged from tens of nanometers to several micrometers, and most were several hundreds of nanometers. Furthermore, by comparison of Figs. 1(b) and (c), we observe that the nanostructure surfaces of the black 1DNSASi sample were relatively smooth. However, most of the internal distances between the adjacent nanostructures of the yellow 1DNSASi sample were several micrometers, and the density of 1D nanostructures was much smaller than that of the black sample (as demonstrated in Figs. 1(d) and (e)). The disparity of colors and morphologies can be accounted for by using the various etching conditions. The black 1DNSASi was fabricated in a 0.2 M H_2O_2 mixed with 4 M HF aqueous solution at room temperature for 30 min, while the yellow sample was fabricated in a 0.4 M H_2O_2 mixed with 4 M HF aqueous solution in a 70 °C water bath for 30 min. In the view of the motility of the metal nanoparticles in Si and induced anisotropic Si etching [22], the Si etching is a redox process, performed at the AgNP/Si interfaces. In the conditions of low oxidant concentration and low reactive temperature, the etching velocity and the area of the Si etching region for given Ag nanoparticles are smaller than those for high oxidant concentration and high reactive temperature. Clearly, the average internal distances and the overall lengths (namely, the etching depth) of the 1D nanostructures of the yellow 1DNSASi sample were larger than those of the black sample.

Figure 2(a) shows the hemispherical optical reflectance spectra of the as-cleaned Si and nanostructured Si. The reflectance of planar Si shows a typical behavior similar to other reports [12,23,24], whereas the reflectance of the black 1DNSASi sample is smaller than 1% over the spec-

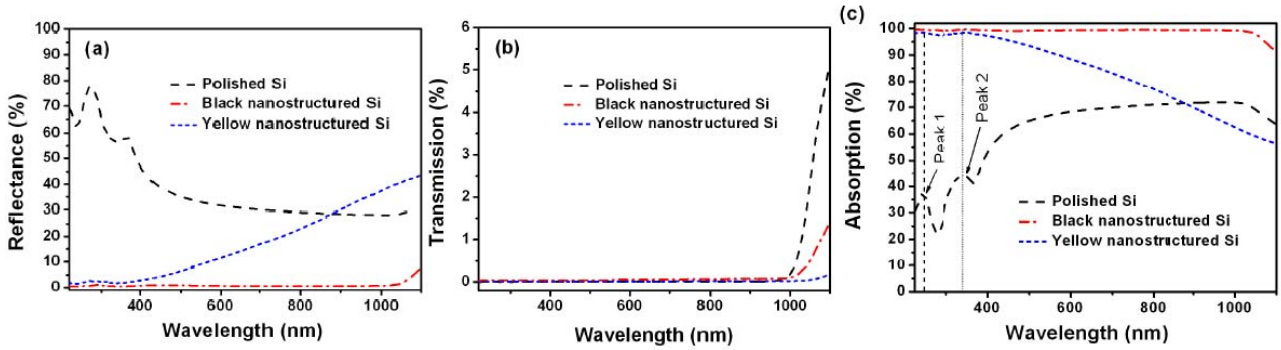

Fig. 2. (Color online) (a) Reflection spectra, (b) transmission spectra, and (c) absorption spectra of planar Si and nanostructured Si with different morphologies.

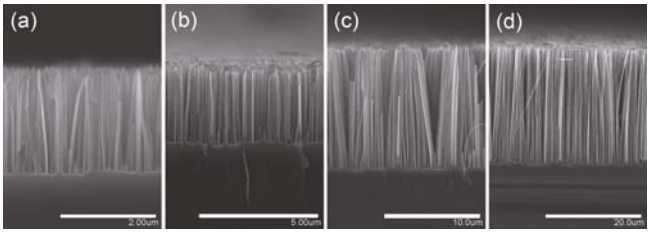

Fig. 3. Cross-sectional SEM images of four kinds of black nanostructured Si fabricated in (a) 5 min, (b) 10 min, (c) 30 min and (d) 60 min.

trum from UV to near IR and exhibits a slow increase at wavelengths above 1030 nm. The ultralow reflectance can be ascribed to the strong light scattering and trapping among the high-density, random and unbroken 1D nanostructures [15]. However, not all the 1DNSASi samples show a low reflectance. The reflectance of the yellow 1DNSASi sample is samller than 3% at wavelengths below 360 nm, but shows a gradual increase at wavelengths above 360 nm, and even become larger than that of the planar Si at wavelengths above 880 nm. This may be due to the internal distances among 1D nanostructures being larger than the wavelength value of incident light and to the combined effects of weak light trapping and strong light scattering, resulting in an increased reflectance with increasing incident wavelength. Moreover, most of the 1D nanostructures in the yellow1DNSASi sample are broken, and the optical absorption of unsmooth and broken 1D nanostructures are usually weakened due to the numbers of breakpoints or opening mouths and to the anisotropy of the optical absorption [25]. Although the etching depth (d) of the yellow sample is much larger than that of the black sample, the densities, distributions and shapes of the nanostructures of the two samples are different, and both depths are much larger than the incident wavelength (λ). Thus, in this instance, the suppression of the reflectance is not positively related to the depth, which disagrees with other research [23, 26], where the reflectance ratio of the etched Si and the polished Si falls exponentially with increasing d/λ value. This may need to determine whether the etching depth is comparable to the incident wavelength.

To further investigate the optical absorption properties of the Si with different nanostructural surfaces, we measured the transmission spectra. Figure 2(b) shows almost zero-transmission for all samples at wavelengths below 1000 nm and a gradual increase in the transmission at wavelengths above 1000 nm, while the overall transmissions are low, and the increasing gradients are different. Planar Si has the greatest rate of increase of the transmission with increasing wavelength while the yellow 1DNSASi sample shows the smallest rate of increase. These phenomena can be attributed to three reasons: 1)The energy of incident light at wavelengths above 1000 nm is smaller than the band gap of Si; 2) the thickness of the Si chips is much larger than the wavelength value of incident light, and the effective thickness is reduced during nanostructuring treatments, so the largest etching depth of the yellow sample indicates the largest transmission and the greatest rate of increase at wavelengths above 1000 nm; 3) nanostructured Si may have a smaller band gap compared to bulk Si, so the nanostructured Si may have a higher wavelength upper limit of light absorption.

The absorption spectra derived from the reflectance and the transmission of the three samples with different morphologies are shown in Fig. 1(c). The black nanostructured Si has a ultrahigh absorption ($> 99\%$) at wavelengths below 1030 nm, and a slow decrease at wavelengths above 1030 nm; the absorption of the yellow sample is also high ($> 97\%$) in the UV spectrum, has a gradual reduction at wavelengths above 400 nm, and is lower than that of the planar Si in the near-IR spectrum. Furthermore, two absorption peaks as designated by the vertical dotted lines can be observed at the same wavelength for all samples. The observations indicate that the intrinsic optical properties of the Si with different morphologies are not modified by the nanostructuring operation, which can be interpreted as the scale of the nanostructure being much larger than the scale of the change in the electronic structure [23,26].

The optical properties of the black 1DNSASi samples

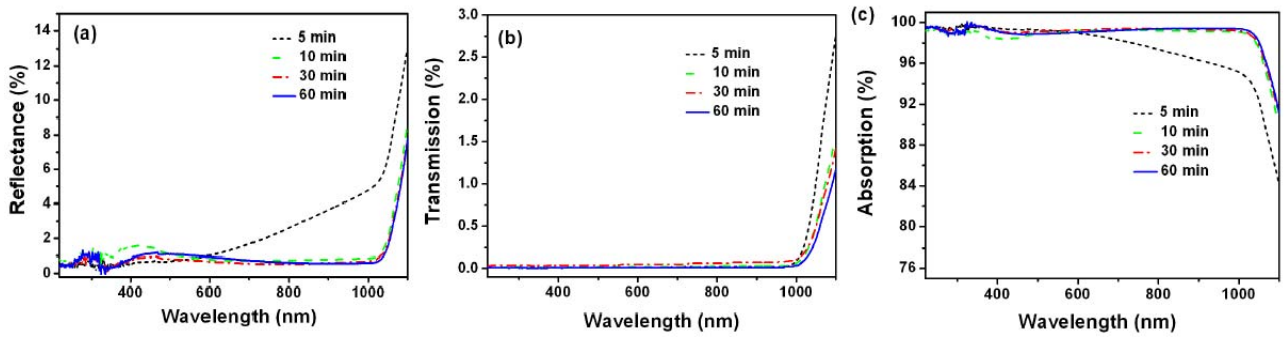

Fig. 4. (Color online) (a) Reflection spectra, (b) transmission spectra, and (c) absorption spectra (calculated from R and T data) of the black nanostructured Si prepared for different etching times.

with various depths prepared in relatively facile conditions for different etching time were studied. Figure 3 shows the cross-sectional SEM images of four kinds of black 1DNSASi samples, and their top-view SEM images are similar to that in Fig. 1(c). From Fig. 3, one can observe that the four samples have similar 1D nanostructures, except for various lengths, which were etched in a mixed solution of 0.4 M HF and 0.2 M H_2O_2 at room temperature for 5, 10, 30 and 60 min, respectively, and the corresponding etching depths were about 2.1, 3.3, 12.5 and 24.8 μm, respectively. Figure 4(a) shows the optical reflectance spectra of the four kinds of black nanostructured Si. As shown in the spectra, all the samples show low reflectance in the UV and the Vis regions. However, the optical reflectance of the 5-min-etched sample shows a slow increase in the wavelength range of 600 - 1030 nm and a rapid increase at wavelengths above 1030 nm, and the other three samples show a similar tendency, namely, a low reflectance in the spectral range of 220 - 1030 nm and a rapidly increasing reflectance at wavelengths above 1030 nm. The reflection properties of the 'moth eye' surface is dependent on the height of the protuberances when the height is smaller or comparable to the wavelength of incident light [15, 16], for the 5-min-etched sample, the etching depth is small and is comparable to the wavelength of visible light, so the reflectance increases with increasing incident light wavelength. Because the etching depths of the other three samples are much larger than the wavelength of incident light, once the light enters into the nanoholes or interspaces among nanostructures, the light will be scattered repeatedly until it is absorbed in or is transmitted out of the sample, and it will not be reflected out of the nanostructures [11]. When the wavelength of the incident light reaches 1030 nm, the energy of the incident light is above the band gap of Si, and light trapping is very limited for all Si structures due to the fact that Si is an indirect-band-gap material and that optical absorption needs photon assistance. This is the reason that the reflectance spectra of Si with different morphologies show an increasing tendency at wavelengths above 1030 nm.

Optical transmission spectra of the four samples are shown in Fig. 4(b). The four samples have similar transmissions-zero transmission at wavelengths below 1000 nm and an increasing tendency at wavelengths above 1000 nm due to the large thickness of Si film and the small energy of the incident photon. Moreover, different transmission spectra are observed for the four samples with different etching depths when the wavelength is over 1000 nm; this observation is due to the effective thickness of the Si thin film being reduced as the etching time increases.

The combined effects of low reflectance and zero transmission in the wavelength region below 1000 nm causes the excellent absorption for the four kinds of black nanostructure-arrayed Si (as shown in Fig. 4(c)). In the wavelength region of 220 - 1000 nm, it is interesting to note that the samples synthesized with larger than 10 min show similar high absorptions ($> 98\%$), independent of the etching depth, while the absorption of the 5-min-etched sample shows a gradual decrease at wavelengths above 600 nm. On the other hand, the absorption rapidly decreases with increasing wavelength over 1000 nm. The absorption of black nanostructured Si can be inferred to be independent of the etching depth when it is larger than a certain value, but when smaller than that certain value, the depth has a significant influence on the optical absorption of the black 1DNSASi sample.

IV. CONCLUSION

The optical properties of two kinds of 1D nanostructure-arrayed Si fabricated under different conditions were investigated, and the nanostrcturing operation not only could enhance but also could weaken the optical absorption, depending on the etching conditions. At a high oxidant concentration and high temperature, the nanostructuring process was drastic, with many unsmooth and broken 1D nanostructures with low density being obtained, and with the nanostructured Si showing a yellow appearance. By adjusting the etching conditions, a black nanostructure-arrayed

Si was obtained, which had ultrahigh absorption (> 99%) at wavelengths below 1030 nm. Furthermore, we demonstrated that the influences of the etching depth on the absorption properties of black nanostructure-arrayed Si: namely, when the etching depth was larger than a certain constant, the absorption reached saturation and was independent of the etching depth. Because of the large surface-to-volume ratio, the few-defect nanostructures and the low-cost preparation, the black 1D nanostructure-arrayed Si has promising applications for photoelectric devices with high efficiency, photodetectors, and sensors with high sensitivity.

ACKNOWLEDGMENTS

This work was supported by the National Basic Research Program of China (No. 2010CB832905) and partially by the Fundamental Research Funds for the Central Universities and the Program for New Century Excellent Talents in University (NCET).

REFERENCES

[1] M. D. Kelzenberg, S. W. Boettcher, J. A. Petykiewicz, D. B. Evans, M. C. Putnam, E. L. Warren, J. M. Spurgeon, R. M. Briggs, N. S. Lewis and H. A. Atwater, Nature Mater. **9**, 239 (2010).
[2] T. T. Zhao, H. Wu, S. Q. Yao, Q. H. Xu and G. Q. Xu, Langmuir **26**, 14937 (2010).
[3] J. B. Han, F. R. Fan, C. Xu, S. S. Lin, M. Wei, X. Duan and Z. L. Wang, Nanotechnol. **21**, 405203 (2010).
[4] S. E. Han and G. Chen, Nano. Lett. **10**, 1012 (2010).
[5] L. H. Zhang, Y. Jia, S. S. Wang, Z. Li, C. Y. Ji, J. Q. Wei, H. W. Zhu, K. L. Wang, D. H. Wu, E. Z. Shi, Y. Fang and A. Y. Cao, Nano. Lett. **10**, 3583 (2010).
[6] H. Kind, H. Q. Yan, B. Messer, A. Law and P. D. Yang, Adv. Mater. **14**, 1580 (2002).
[7] M. D. Kelzenberg, D. B. Evans, B. M. Kayes, M. A. Filler, M. C. Putnam, N. S. Lewis and H. A. Atwater, Nano. Lett. **8**, 710 (2008).
[8] G. J. Zhang, J. H. Chua, R. E. Chee, A. Agarwal, S. M. Wong, K. D. Buddharaju and N. Balasubramanian, Biosens. Bioelectron. **23**, 1701 (2008).
[9] S. Sen, P. Kanitkar, A. Sharma, K. P. Muthe, A. Rath, S. K. Deshpanda, M. Kaur, R. C. Aiyer, S. K. Gupta and J. V. Yakhmi, Sens. Actuators B **147**, 453 (2010).
[10] Y. Ahn, J. Dunning and J. Park, Nano. Lett. **5**, 1367 (2005).
[11] H. Lu and C. Gang, Nano. Lett. **7**, 3249 (2007).
[12] S. Koynov, M. S. Brandt and M. Stutzmann, Appl. Phys. Lett. **88**, 203107 (2006).
[13] M. F. Chen, H. C. Chang, A. S. P. Chang, S. Y. Lin, J. Q. Xi and E. F. Schubert, Appl. Opt. **46**, 6533 (2007).
[14] E. Yablonovitch and G. D. Cody, IEEE Trans. Electron. Devices **29**, 300 (1982).
[15] P. B. Clapham and M. C. Hutley, Nature **244**, 281 (1973).
[16] S. J. Wilson and M. C. Hutley, J. Mod. Opt. **29**, 993 (1982).
[17] S. S Oh, C. G. Choi and Y. S. Kim, Microelectron. Eng. **87**, 2328 (2010).
[18] C. Lee, S. Y. Bae, S. Mobasser and H. Manohara, Nano Lett. **5**, 2438 (2005).
[19] A. V. Shah, M. Vanecek, J. Meier, F. Meillaud, J. Guillet, D. Fischer, C. Droz, X. Niquille, S. Fay, E. Vallat-Sauvain, V. Terrazzoni-Daudrix and J. Bailat, J. Non-cryst. Sol. **639**, 338 (2004)
[20] S.-L. Wu, T. Zhang, R.-T. Zheng and G.-A. Cheng, Chem. Phys. Lett. **538**, 102 (2012).
[21] S.-L. Wu, T. Zhang, R.-T Zheng and G.-A. Cheng, Appl. Surf. Sci. **258**, 9792 (2012)
[22] K. Q. Peng, A. J. Lu, R. Q. Zhang and S. T. Lee, Adv. Funct. Mater. **18**, 3026 (2008).
[23] H. M. Branz, V. E. Yost, S. Ward, K. M. Jones, B. To and P. Stradins, Appl. Phys. Lett. **94**, 231121 (2009).
[24] L. Tsakalakos, J. Balch, J. Fronheiser, M. Y. Shih, S. F. LeBoeuf, M. Pietrzykowski, P. J. Codella, B. A. Korevaar, O. Sulima, J. Rand, A. Davuluru and U. Rapol, J. Nanophotonics **1**, 013552 (2007).
[25] Y. Ahn, J. Dunning and J. Park, Nano Lett. **5**, 1367 (2005).
[26] K. Hadobas, S. Kirsch, A. Carl, M. Acet and E. F. Wassermann, Nanotechnol. **11**, 161 (2000).